Fluid inclusion and geochemical evidence for fluid mixing in the genesis of Ba–F (Pb–Zn) lodes of the Spanish Central System

F. TORNOS,[1] C. CASQUET,[2] J. LOCUTURA,[1] AND R. COLLADO[2]

[1] Instituto Tecnológico Geominero de España, Rios Rosas 23, 28003 Madrid, Spain

[2] Facultad de Ciencias Geológicas, Universidad Complutense, 28004 Madrid, Spain

Abstract

Fluid inclusion data and geochemical evidence lead to a genesis of Ba–F (Pb–Zn) lodes of the Spanish Central System as related to fluid mixing of hot (>300 °C), low saline (<0.6 molal), Na–K deep fluids and cool (<100 °C), oxidized, more saline (>2.8 molal), Na–K–Ca–Mg brines of phraeatic origin. Ore formation took place at relative low depth and temperatures (from 270 to 120 °C) in a regime of increasing f_{O_2}, (Ca + Mg)/Na ratio and pH of the fluids towards the surface. Such evolution destabilizes the chloride metal complexes, allowing for the precipitation of Zn and Pb carried by the deep solution.

Vertical fluorite-baryte zonation is explained in terms of mineral solubilities. Fluorite deposition in the deeper mineralized zone is related to a slight increase of mCa^{2+} of the fluid in the lower part of the fluid mixing zone; further increase of mCa^{2+} and mMg^{2+} towards the surface promotes fluorite dissolution. Increase of f_{O_2} in the shallow part of the hydrothermal system promotes the oxidation of ΣH_2S to $\Sigma SO_4^{=}$, resulting in baryte formation.

We propose an ore genesis related to fluid mixing in shallow hydrothermal systems associated with an extension of Permo–Triassic age. Such interpretation is in agreement with the present day ideas for the genesis of many of the Ba–F deposits in the Hercynian Belt of Europe.

KEYWORDS: fluid inclusions, fluid mixing, Ba-F lodes, Spanish Central System.

Introduction

OVER thirty mines, mostly inactive at present, have been mined for Pb–Zn and Ba–F in the western part of the Spanish Central System, a massif that makes part of the inner zone (Centro Iberian Zone) of the Hercynian Belt of Spain (Fig.1). Most lodes are hosted by peraluminous porphyritic adamellites and minor leucogranites (347 to 310 Ma and 291 to 288 Ma in age respectively; Ibarrola *et al.*, 1988). Sometimes they cut across high-grade metamorphic rocks, usually orthogneisses (Fig. 1).

The lodes follow two systems of brittle faults, N60° to 70°E and N110° to 120°E in trend, that are the result of a late-Hercynian reactivation of earlier strike–slip faults that evolve in time from ductile-brittle to brittle in behaviour. On a larger scale, these faults seem to be concentrated along a regional North–South-trending zone of structural weakness (Ubanell, 1981), similar to those found elsewhere in the Hercynian Belt of Europe (Routhier, 1983). These faults show a complex hydrothermal alteration, with an earlier quartz leaching accompanied by feldspar precipitation (episyenites; Tornos, 1990) followed by an acid alteration (quartz–muscovite–chlorite, with minor adularia) related to quartz veins. F–Ba lodes are linked to a late brittle reactivation and fill-dilatancy zones along the faults; the relative chronology of the faults suggests that those lodes are Permo-Triassic in age (Ubanell, 1981; Locutura and Tornos, 1987).

The lodes are very irregular in form showing, as a rule, a short vertical extension of 100–200 metres, and a thickness less than 2–3 metres. They can be several kilometres in length, with discontinuous mineralization along the structure. Ore-rich bodies, with increase in thickness and ore grade, are found at dilatanty zones of the faults or wherever the two groups of fractures intersect. Internal structure is usually brecciated, but rhythmic banding is also locally found. On the basis of geological data, four zones, that are

Mineralogical Magazine, June 1991, Vol. 55, pp. 225–234

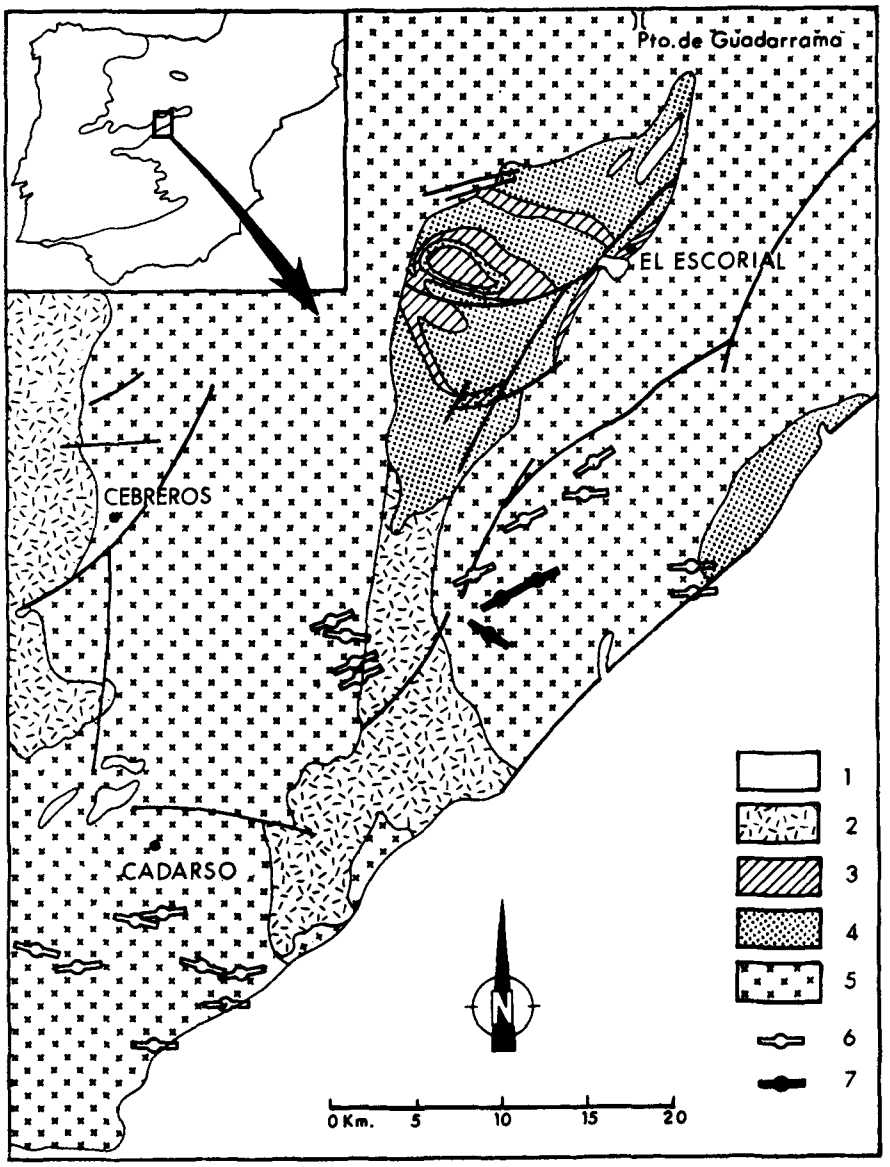

FIG. 1. Geological setting of mineralizations. (1) Cacnozoic sediments; (2) Schists and gneisses (Precambrian?); (3) Femic paragneises and augen gneises (Precambrian?); (4) Orthogneisses (Cambrian-Ordovician); (5) Adamellites and granites; (6) Baryte lodes; (7) Fluorite–baryte lodes.

different in terms of age and depth, are distinguished: (A) a deeper and earlier Acidic Zone, characterized by the alteration of the host granites with destruction of micas and feldspars to sericite, quartz and chlorite; (B) a Fluorite Zone; (C) a Fluorite + Baryte Zone, where fluorite and baryte coexist; and (D) a shallower and younger Baryte Zone. In the last three zones, a vertical and lateral zonation is well displayed, with fluorite in the deepest and outer parts and baryte in the shallowest and inner parts of the lodes. Quartz is widespread and carbonates, calcite and ankerite, are common as late fillings.

Metallic minerals are found in veins or pods along with quartz, fluorite or baryte. Galena is the most abundant, whilst Fe-poor sphalerite (M_{FeS}

= 0.2–2) is scarce, particularly in the upper baryte-rich parts. Other minerals are pyrite, chalcopyrite, freibergite (as inclusions in galena), bismuthinite, native bismuth, pearceite and gersdorffite (Vindel, 1980; Locutura and Tornos, 1987; Mayor *et al.*, 1988; Ortega *et al.*, 1988).

Hydrothermal alteration is restricted to the proximity of the lodes. Silicification, sericitization and local chloritization are the usual alterations related to the deeper Acidic Zone and Fluorite Zone, while argillization (smectite formation) is widespread in the upper zones of the hydrothermal system (Mayor *et al.*, op. cit.). These alterations locally overprint an older hydrothermal history, associated with an older activity of the faults, that gave rise to episyenites and a later acidic alteration (silicification, sericitization and chloritization). Minute grains of pyrite and chalcopyrite are found disseminated in these hydrothermally altered host rocks. Supergene alteration of the lodes gives rise to cerussite, anglesite, goethite, marcasite, chalcocite, covelline and smithsonite along with kaolin. Complementary analytical data of rocks and minerals can be found in Locutura and Tornos (op. cit.).

In an earlier work, Vindel (1980) linked these F–Ba mineralizations with the outermost zone of a periplutonic hydrothermal around the 'La Cabrera' granitic massif, that is some 40 km to the east. Afterwards, Martinez *et al.* (1988) and Ortega *et al.* (1988) reinterpreted the lodes as formed by an epithermal fluid derived from an underlying granite. Ortega *et al.* (op. cit.) proposed that Ba-rich fluids were exsolved from the magma before biotite crystallization. In contrast with these views, Locutura and Tornos (1985, 1987) proposed an origin by mixing of ascending deep meteoric fluids with shallow waters.

The aim of this paper is to interpret the evolution of the hydrothermal system on the basis of fluid-inclusion data and theoretical thermodynamic calculations to clarify the mechanisms of ore precipitation and vertical fluorite–baryte zonation in this type of mineralization.

Fluid inclusion data

Fluid inclusion work has been carried out on selected samples collected *in situ* at the San Eusebio and Asturiana mines (Colmenar de Arroyo, Madrid); a total of 69 and 42 fluid inclusions have been studied in fluorite and baryte respectively. Interpretation of fluid inclusion data has been done with a modified version of the program HALWAT by Nicholls and Crawford (1985).

Following criteria given by Roedder (1984), fluid inclusions interpreted as primary are quite scarce and small, usually between 2 and 10 μm in size. They are found in fluorite and to a lesser extent in baryte and quartz, and are monotonous in composition. They consist of a brine and a small gas bubble which never exceed 30 per cent of the volume. Two types of secondary fluid inclusions are also found; water-rich inclusions, similar to the primary ones, and very small (less than 2–3 μm) CH_4–CO_2-rich inclusions that cut the previously cited minerals along microfractures. Since these secondary fluid inclusions are younger than the main minerals of the lodes, their importance in the ore genesis in considered minimal and therefore they will not be considered any further in this work.

Primary fluid inclusions in fluorites show higher homogenization temperatures (T_h), in the range 270–150 °C, and last melting temperatures of ice (T_m) between −7 and 0 °C (0–10.5% NaCl eq.), with a maximum between −4 and −1 °C; an average value of 3.4% NaCl eq. (i.e. $T_m = -2$ °C) has been choosen for further calculations (Fig. 3 and Table 2). Fluid inclusions in baryte are usually more saline, with lower final melting temperatures (−10 to −2 °C, 3.4–14% NaCl eq.) with a maximum between −7 and −6 °C, and also lower homogenization temperatures (200–120 °C). Recorded first melting temperatures are near −20 to −22 °C in the less saline inclusions, whilst in the more saline ones they reach values of −38 to −52 °C. This evolution is well displayed by the trend shown in Fig. 2, corresponding to a single sample where older fluorite shows higher homogenization temperatures and higher melting temperatures of ice than younger baryte. Fluid inclusions in quartz older than the mineralization yield still higher homogenization temperatures (260–300 °C) and final melting temperatures ($T_m > -2$ °C).

Absence of clathrate and of detectable insoluble bubbles in glycerine under the crushing stage in fluid inclusions of all the hydrothermal zones, limits the X_{CO_2} in the fluid to less than 0.01 (Hedenquist and Henley, 1985, Ulrich and Bodnar, 1988). Presence of calcite and ankerite in the latter stages of mineralization along with thermodynamic considerations based on equilibrium constants by Fournier (1985*b*), also suggest that X_{CO_2} was very low, in the range 0.010 to 0.015 at this late stage. Such low molality of CO_2 (0.28 to 0.52 molal) in the fluids has a little effect on the salinity correction; depression of T_m (Hedenquist and Henley, 1985) is near 1 °C in fluid inclusion from barites and even less in fluorites.

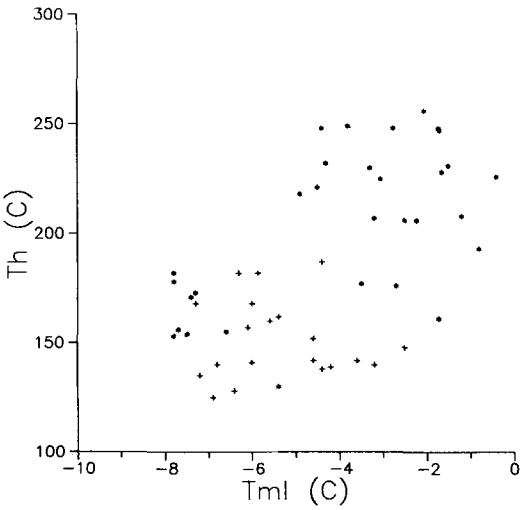

FIG. 2. Correlation between melting temperatures of ice and homogenization temperatures of fluorite and baryte in a selected sample. (*) Fluid inclusions in fluorite. (+) Fluid inclusions in baryte. Secondary fluid inclusions in fluorite have lower melting temperatures of ice and lower homogenization temperatures than primary fluid inclusions.

Selected samples of quartz from the Acidic Zone, fluorite and early and late baryte were crushed into chips 3–5 mm in size and washed under boiling distilled water. Then they were heated to 600 °C in a furnace to assure complete decrepitation of fluid inclusions. Salts precipitated at the surface by the escaping fluids (decrepitates) are then removed with boiling distilled water and taken for Ca, Na, K and Mg analysis by atomic absorption spectrometry. Results are shown in Tables 1 and 2, and as Na/K/(Mg + Ca) ratios in Fig. 4. Although problems like mixing of decrepitates from different generations of fluids and some contamination due to mineral inclusions (Bottrell *et al.*, 1988) can occur, the results (Table 1) are in agreement with the microthermometric data.

Interpretation of such analyses in the terms of equilibrium–disequilibrium with the quartz–muscovite–feldspar buffer, as proposed by Giggenbach (1988), show that the hydrothermal fluid has a complex evolution (Fig. 4). Theoretically calculated values for Na/K relationship following the method of Henley *et al.* (1984) using equilibrium constants from SUPCRT (Helgeson *et al.*, 1978) show that fluids in the Acidic Zone are high K/Na, low Ca and Mg immature waters (Giggenbach, op. cit.) in disequilibrium with granite (Na/K ratio for Q–Ms–Kf–Ab of 0.20/0.02, in the solution 0.11/0.10, Table 2). They are partly equilibrated with the granite during fluorite precipitation with increase of the Na proportion (Na/K ratio for Q–Ms–Kf–Ab of 0.21/0.02, of solution 0.20/0.01). However, baryte is related to a progressive increase of the (Ca + Mg)/(Na + K) and K/Na proportions in the fluid (Fig. 4, Table 2), showing a complete disequilibrium with the enclosing rocks. Iron contents are very low, close to the detection limit (about 0.01 m).

Genetic model

All the fluid inclusions studied homogenize to the liquid phase. However, the presence of local breccias with a chlorite–adularia–quartz matrix in the Acidic Zone can be only interpreted as resulting from a pH increase due to degassing by boiling of the system (Reed and Spycher, 1985). Lack of fluid inclusions homogenizing to vapour can be explained by incomplete sampling or, as explained by Roedder (1984), to quick escape of steam towards the surface in shallow hydrothermal systems. Coincidence between homogenization temperatures and temperatures found by chlorite and sericite geothermometry (325–342 °C and less than 250 °C respectively; Locutura and Tornos, 1987) suggest that T_h and trapping temperature were very similar during the Acidic Stage. If boiling or close to boiling conditions are assumed, homogenization pressures of 39 to 85 bars can be calculated for these low-salinity fluids with the equations of liquid–vapour curve in Henley *et al.* (1984); such values correspond to an equivalent depth of 460–1100 metres if the system is opened to the surface; if the system is a closed one, such boiling pressures can be reached assuming a rock density of 2.8 g/cm^3 and fluid pressure to be similar to a lithostatic one, between 139 and 318 m depth. Probably true pressures are between such values, because shallow hydrothermal systems are usually partially connected to the surface. No evidence of boiling has been found in shallower zones suggesting a progressive departure of the fluid from the boiling curve; this fact can be only explained by a density increase upwards in the hydrothermal column linked to a quick cooling of fluids or/and an increase in their salinity (Table 2).

However, boiling alone cannot explain the previously discussed chemical evolution of the fluid, with an important increase of salinity (from less than 0.6 molal to near 14 molal) and change in the relative proportions of the main components. Furthermore, during early boiling at the Acidic Stage, little ore deposition took place as only minor pyrite and chalcopyrite are found

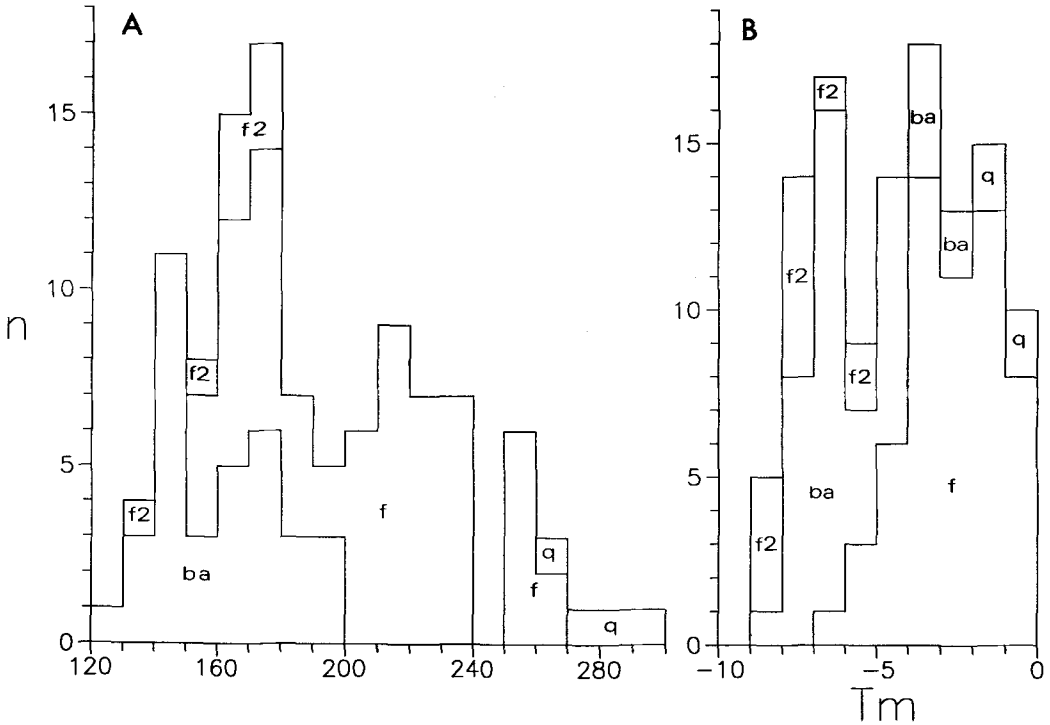

FIG. 3. (A) Homogenization temperatures and (B) last melting temperatures of ice of fluid inclusions in quartz of the Acidic Zone (q), primary fluid inclusions in fluorite (f), primary inclusions in baryte (ba), and secondary inclusions in fluorite (f2).

within these rocks; since this mechanism is very effective for ore deposition in hydrothermal systems (Reed and Spycher, 1985), absence of significative mineralization suggests that fluids were metal-poor.

TABLE 1. Analyses of leachates of the Acidic Zone (Quartz), Fluorite Zone (Fluorite) and Fluorite + Baryte and Baryte Zones (Baryte) in parts per million. Analysed values for Fe are close to the detection limit. Sample B-6 is of quartz in the Baryte Zone. Total salinities estimated from mean values of melting temperatures of fluid inclusions of each stage assuming that $m_{total} = m$NaCl equiv.

Sample	Mineral	Na	K	Ca	Mg	Fe	m_{total}
Q-2	Quartz	1.14	1.42	---	0.12	0.40	0.23
Q-3		1.02	1.70	---	0.15	0.52	0.23
F-1	Fluorite	15.74	1.02	3.64	0.06	0.27	0.23
F-2		15.00	0.93	2.15	0.04	0.22	0.23
F-3		27.58	1.03	3.91	0.05	0.14	0.23
B-1	Barite	14.50	10.69	13.78	5.38	0.11	2.01
B-2		10.22	1.70	1.54	0.90	0.11	0.60
B-3		8.27	2.31	2.13	2.20	0.36	0.60
B-4		4.28	4.14	2.78	2.91	---	2.01
B-5		6.96	14.97	2.78	3.58	---	2.01
B-6		6.86	1.54	7.26	0.23	---	2.01

Theoretical calculations by Reed and Spycher (op. cit.) show that simple cooling of a low-saline hydrothermal fluid should give rise to progressively more acidic waters and therefore should precipitate no other ore minerals than pyrite; also, the presence of fluorite, baryte and carbonates excludes cooling as a depositional mechanism, because the solubility of these minerals increases with a drop in temperature (Blunt, 1977; Richardson and Holland, 1979; Fournier, 1985*b*).

Excluding simple cooling and boiling as the main mechanisms involved in ore deposition, the only mechanism that can produce at the same time a significant drop in the temperature and an increase in salinity with an important chemical change of the fluid, with associated ore precipitation, is the mixing of two different fluids, that should correspond to the end-members found in the system; a deep and low-salinity (0–0.6 molal), high-temperature (>300 °C), Ca-poor brine and an oxidized, more saline (>3 molal), denser (0.9–1 g/cm^3) and cooler (<100 °C) fluid, with high relative contents of Ca, Mg and K.

The main characteristics of each Zone are contained in Table 2. They have been established

TABLE 2. Mean fluid inclusion data and calculated pH for the different zones in the hydrothermal evolution of mineralization. Values in brackets are mean values used for calculations except in Na and K molalities that represent the theoretical Na and K contents of a fluid of the same total salinity in equilibrium with the quartz–muscovite–feldspars buffer. Concentration of ionic species in fluid are recalculated to mNa(eq) = mNa + mK + mCa + mMg.

	T°C	Prof (m.)	%NaCl eq.	dens	mNa	mK	mCa	mMg	XCO2	pH	logfO2	logfS2	mΣS
Acidic Zone (A)	260–300 (300)	140–1100 (P=L-V)	0–3.4% (1.3)	0.7–0.8	0.11 (0.20)	0.09 (0.03)	0.00	0.01	<0.005	2.89–4.97 (4)	–33	–10	0.005
Fluorite Zone (B)	180–270 (250)	>115 (P>L-V)	0–10.5% (1.3)	0.72–0.99	0.20 (0.21)	0.01 (0.02)	0.02	0.01	<0.005	3.09–5.07 (5)	–36	–11	0.005
Fluorite–Barite Zone (C)	200	>77	3.4	0.89	0.43	0.05	0.05	0.07	<0.01	5	–39	–11.3	0.003
Barite Zone (D)	130–200 (150)	>>20 (P>>L-V)	3.4–13.9% (10.5)	0.89–1.03	0.66	0.63	0.44	0.29	<0.01	5	–46	–18	0.001

on the basis of fluid-inclusion data (Fig. 3), paragenesis, and theoretical considerations. The pH values were estimated from the Na/K ratio of the fluid inclusions and from equilibrium constants of quartz–moscovite–feldspar equilibria as discussed by Henley *et al.* (1984). Absence of K-feldspar and kaolin limit pH of quartz–moscovite association at the ranges shown in Table 2. The pH evolution is probably the result of the progressive equilibration of the deep inflowing acid fluids (pH ≈ 4) with the quartz–moscovite–feldspar association in the host granite; full equilibration was achieved during fluorite formation (pH ≈ 5, Table 2). Finally, fluids in the Baryte Zone are neutral to slightly alkaline (5.5–6) as suggested by the ankerite precipitation and high Ca and Mg contents of the fluid.

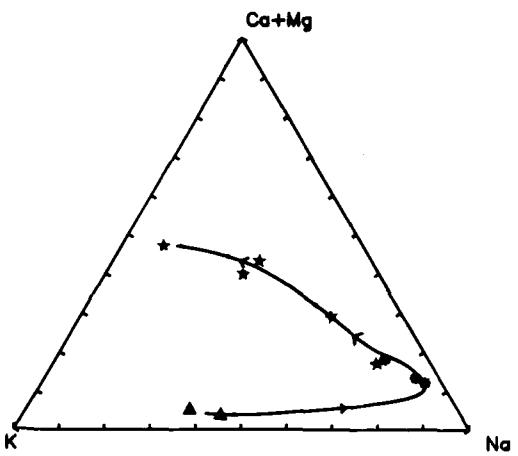

FIG. 4. Representative major cation proportions (in weight) in the fluid inclusions. (▲) Quartz of the Acidic Zone, (*) Fluorite, (#) Baryte. Solid line and arrows show chemical trend of deep fluid by mixing with the shallower one.

The total sulphur ($m\Sigma S$) content of the fluid has been roughly estimated from mineral equilibria in f_{O_2}–f_{S_2}–pH space (Locutura and Tornos, 1987) to be near 0.005 molal during the formation of the earlier and deeper Acidic and Fluorite Zones. The absence of bornite, hematite, and anhydrite in the Baryte Zone suggest that, for a pH between 5.5 and 6, $m\Sigma S$ should be very low; therefore, a value of 0.001 $m\Sigma S$ was assumed for theoretical calculations.

The evolution of the hdyrothermal system can be shown on an f_{O_2}–pH diagram (Fig. 5) on the basis of the chlorite–pyrite–quartz association (Walshe, 1986; Locutura and Tornos, 1987) in the Acidic Zone (A), sphalerite + pyrite association in the Fluorite Zone (B) and sphalerite + pyrite + bismuthinite + bismuth association (Barton and Skinner, 1979) in the Baryte Zone (D). Evolution from (B) to (D) is a continuous one, the Fluorite + Baryte Zone (C) representing an intermediate stage. Since no decrepitate analyses are available for this latter stage, its fluid composition has been estimated by interpolation between (B) and (D), assuming that fluid inclusions in baryte with higher T_h and lower T_m probably correspond to this stage. As can be seen in Fig. 5, fluid evolution towards the upper zones of the hydrothermal system is characterized by an increment of f_{O_2} and slight increase in alkalinity, whilst in the deeper parts acidic and reduced conditions are found.

Transport and precipitation of minerals in the hydrothermal system

The solubility of aqueous species of major interest in the hydrothermal fluids has been modelled with a computer program based on equations by Helgeson *et al.* (1978) and Henley

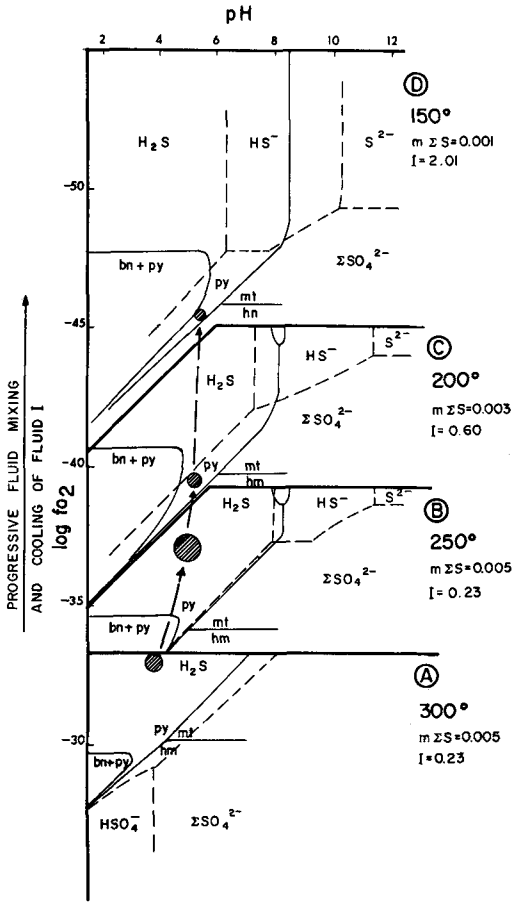

FIG. 5. log f_{O_2}-pH evolution of fluids. Discontinuous lines are fields of stability of different sulphur species. Continuous lines are stability fields of representative minerals of the system Cu–Fe–S–O. $m\Sigma S$ is total dissolved sulphur as calculated in the text and I is the ionic strength of fluids. Shaded circles and arrows show the evolution of deep fluids by mixing with the shallower ones.

TABLE 3. Solubility (in mg/kg) of F, Pb, Zn and Cu in equilibrium with fluorite, galena, sphalerite and chalcopyrite + pyrite respectively with speciation of the major soluble complexes at conditions defined in Fig. 5 and Table 2.

		A	B	C	D
Fluorite solubility	CaF^+		88%	66%	93%
	HF		6%	1%	
	F^+		3%	2%	
	MgF^+		2%	30%	7%
	NaF		1%		
		>100	12	17	41
Galena solubility	$PbCl_2$	56%	35%	4%	2%
	$PbCl_3^-$	38%	8%	3%	2%
	$PbCl^+$	6%	9%	2%	
	$PbCl_4^=$			1%	9%
	$Pb(HS)_2$		4%		8%
	$Pb(OH)^+$		2%		
		1106	0.16	0.31	0.23
Sphalerite solubility	$ZnCl_2$	12%	8%	11%	1%
	$ZnCl^+$	29%	41%	52%	2%
	$ZnCl_4^{2-}$	59%	4%	22%	61%
	$Zn(HS)_2$		8%		1%
	$Zn(OH)^+$		2%	4%	
	Zn(HS)(OH)		31%	11%	33%
		1458	0.45	0.79	0.17
Chalcopyrite solubility (+pyrite)	$CuHS_2^-$	92%	100%	100%	100%
	$CuCl_2^-$	5%			
	CuCl	2%			
		77	473	88	>10000

et al. (1984). Activity coefficients of ions have been calculated with the modified Debye–Hückel equation proposed by Helgeson *et al.* (1981) with parameters A and B and effective ionic radii taken from Helgeson (1969) and Henley *et al.* (op. cit.). Equilibrium constants are derived from the previous authors, and also from Blount (1977), Bourcier and Barnes (1987), Fournier (1985*a*), Patterson *et al.* (1981), Richardson and Holland (1979) and Seward and Barnes (1987).

Mineral saturation equilibria at ionic strengths constrained by fluid-inclusion data (Table 3) show that fluorite is very soluble (up to 130 ppm) as HF and to a lesser extent as F^- and NaF under acid (pH ≈ 4) and high-temperature (>200 °C) conditions; precipitation in the Fluorite Zone is triggered by a combination of fluid cooling and an increase of pH and Ca^{2+} activity (Fig. 6), that destabilizes the HF complex. However, a further increase of the ionic strength of the fluids and of Ca^{2+} and Mg^{2+} activities in the upper parts of the hydrothermal system (Baryte Zone) decrease the fluorite precipitation due to rapid formation of CaF^+ and MgF^+ complexes.

However, baryte precipitation can be related to an increase of the $\Sigma SO_4^=/\Sigma H_2S$ ratio of fluids owed to the high f_{O_2} in the shallower Baryte Zone (Fig. 6). Since baryte is one of the most insoluble minerals in oxidized systems (Richardson and Holland, 1979), its precipitation defines clearly the zone of mixing of reduced fluids, containing Ba and/or S, with highly oxidized ones. Low dissociation constants of baryte (Blount, 1977) promotes this precipitation even with very low contents of Ba and S in the fluid. The absence of anhydrite is explained as it is at least 1000 times more soluble than baryte (Patterson *et al.*, 1981) and therefore needs higher concentrations of Ca

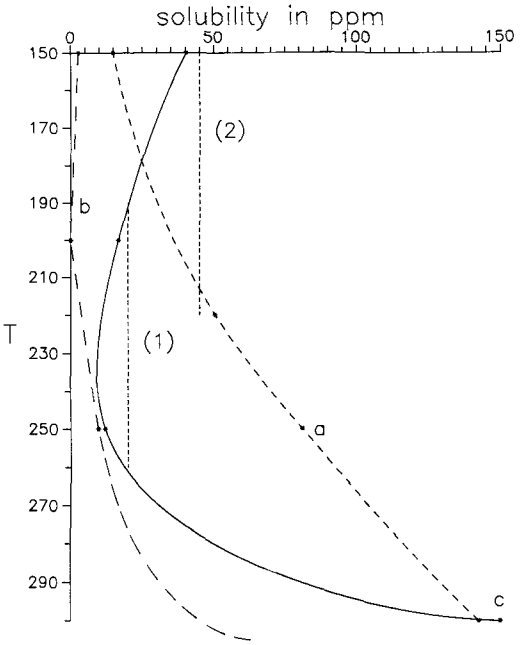

FIG. 6. Solubilities of gangue minerals in conditions defined in Fig. 5 and Table 2. (a) Quartz, (b) Baryte, (c) Fluorite. (1) represents the temperature interval at which fluorite precipitates and (2) the interval of precipitation of baryte.

and S to form. Quartz can form throughout the entire hydrothermal system (Fig. 6).

At the conditions established for this hydrothermal system, transport of Zn and Pb takes place mainly as chloride complexes, whilst copper is transported as thiosulphide complexes (Table 3). The deeper low-salinity fluids have a considerable transport capability, as much as more than 1000 ppm of Zn and Pb and near 80 ppm of Cu at 300 °C. Galena and sphalerite precipitation occur due to oxidation and increase in pH and, to a lesser extent, rapid cooling, due to mixing of the two fluids. Such processes lower the solubility of Zn and Pb to less than 1 ppm (Fig. 7), promoting mineral precipitation even from fluids with very low metal concentrations. Solubility trends of copper are more irregular, in agreement with the low Cu/(Zn + Pb) ratios of these mineralizations.

Discussion

F–Ba lodes similar to those described here are found elsewhere in the Hercynian Basement of the Iberian Peninsula (Melgarejo and Ayora, 1985; Canals and Ayora, 1988; Tritlla and Cardellach, 1988; Locutura *et al.*, 1990) and Europe (e.g. Lhegu *et al.*, 1982; Thibieroz, 1982; Dill, 1988). Almost all of them display the same vertical zonation, with fluorite at depth and baryte in the highest parts. At some places (e.g. Mina Atrevida, Tarragona, Spain) they are found cutting across Permo-Triassic sediments (Melgarejo and Ayora, op. cit.), but they are always covered by the Muschelkalk. Close to the lodes, baryte cements in the basal levels of the Permo-Triassic conglomerates are common.

The two fluids involved in the genesis of the F–Ba veins of the Spanish Central System are probably of two distinctive origins. Low-salinity Na–K acid fluids are similar to the ones described in other hydrothermal systems of the Spanish Central System, as deep meteoric waters involved in hydrothermal convective cells and responsible for the formation of Cu, Zn, Pb, W and Sn replacement and vein mineralizations (Tornos, 1990). On the other hand, the characteristics of the low-temperature, higher salinity, oxidized, and complex brines are compatible with a phraeatic origin of the fluids, probably derived from the water table of the extensional Permo-Triassic basins that descended along the most permeable zones. In fact, in active geothermal systems, the bottom of the groundwater table can be as deep as 400 m (De Ronde and Blattner, 1988). Vertical

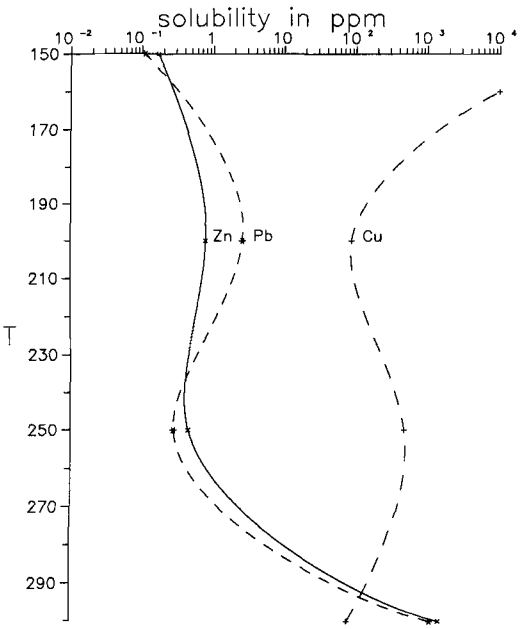

FIG. 7. Solubilities of ore minerals in conditions defined in Fig. 5 and Table 2. (*a*) Zn in equilibrium with sphalerite; (*b*) Pb in equilibrium with galena; (*c*) Cu in equilibrium with pyrite and chalcopyrite.

evolution of fluids in this hydrothermal system shows a trend inverse to that of typical geothermal fields, where deep fluids are diluted by less saline shallow waters (McKibben *et al.*, 1988). This fact could be explained by the common occurrence of sabkha paleogeographic conditions in Permo-Triassic times (Melgarejo and Ayora, op. cit.), thus allowing for the existence of alkaline, high-salinity ground waters.

Geochemical data from Locutura and Tornos (1985) and Tornos (1990) show that 10–210 ppm Pb, 55–465 ppm Zn, 10–80 ppm Cu, 116–125 ppm F and an average of 440–490 ppm Ba contained in the granites of the Spanish Central System are redistributed during the acid alteration along faults due to the destruction of feldspar and micas. This process can easily incorporate some tens of ppm of Pb, Zn, Cu and F to a low-salinity brine (Table 3). As has been shown, theoretical prediction of evolution of hydrothermal systems, such as the one proposed here, can explain precipitation of metals even from very dilute fluids (e.g. 5 ppm Ba, 10 ppm F, and less than 10 ppm of Zn and Pb), without resorting to any metal preconcentration.

Ba and S transport seems to be more complex; the presence of baryte in red beds of Permo-Triassic age in other areas (e.g. Melgarejo and Ayora, 1985) and isotopic data (Canals *et al.*, 1988), along with the impossibility of Ba and S being transported in oxidized shallow fluids (e.g. Blount, 1977), suggest that these elements were carried by the deep fluids.

Conclusions

Fluid-inclusion data, along with geological observations and theoretical prediction of metal solubilities in hydrothermal systems explain the genesis and zonation of Ba–F (Pb–Zn) lodes of the Spanish Central System. Such mineralizations represent the evidence of old hydrothermal meteoric systems. In them, ore precipitation took place by mixing of slightly acid, Na–K low salinity fluids equivalent to chloride waters of active geothermal systems (e.g. Giggenbach, 1988) and phraeatic, oxidized and more saline Na–K–Ca–Mg brines probably related with paleosurfaces and Permo-Triassic in age.

Late to post-Hercynian, brittle extension faults are pathways for such fluid convective cells. Their genesis might be related to the conductive cooling of granites and in the later stages (below 250 °C), given out by radioactive decay of K, U and Th in granites (Fehn, 1985).

Mixing of the deep fluid with the shallower one, lowers temperature and raises f_{O_2} and to a lesser extent pH promoting destabilization of chloride complexes allowing for the precipitation of sphalerite and galena. Vertical fluorite–baryte zonation in the lodes is explained by an increase, towards the surface of $a{Ca^{2+}}/a{H^{+2}}$, $a{Mg^{2+}}/a{H^{+2}}$ and f_{O_2} in the hydrothermal system. Whilst fluorite is stable under low Ca^{2+} molalities of the fluids, i.e. in the deepest part of the fluid mixing zone, baryte is found closer to the surface where oxidized species of sulphur are dominant.

Acknowledgements

This work has been carried out during the surveying for project 'Mapa Metalogénico de España, Hojas 1/200000 numeros 38 y 45' of the Instituto Tecnológico GeoMinero de España (ITGE) (J. Locutura, F. Tornos). We are grateful to the ITGE for the analytical support. This work has also benefited from financial support of C. Casquet, F. Tornos and R. Collado through the CICYT research project 'Actividad hidrotermal tardihercínica del Sistema Central Español' (PB 88-0124). We are indebted to an anonymous reviewer for constructive criticism.

References

Barton, P. B. and Skinner, B. J: (1979) Sulfide Mineral stabilities. In *Geochemistry of Hydrothermal Ore Deposits* (Barnes, ed.), 2nd edition. Wiley and Sons, New York, 278–403.

Blount, C. (1977) Barite solubilities and thermodynamic quantities up to 300 °C and 1400 bars. *Amer. Mineral.*, **62**, 942–57.

Bottrell, S. H., Yardley, B., and Buckley, F. (1988) A modified crush leaching method for the analysis of fluid inclusion electrolytes. *Bull. Mineral.*, **111**, 279–90.

Bourcier, W. L. and Barnes, H. L. (1987) Ore solution chemistry: VII. Stabilities of chloride and bisulfide complexes of zinc to 350 °C. *Econ. Geol.*, **82**, 1839–63.

Canals, A. and Ayora, C. (1988) Las mineralizaciones filonianas del sector de l'Argentera (Cadenas Costero Catalanas): Contexto geológico, estructura, tipología y condiciones de formación. *Acta Geol. Hisp.*, **23**, 155–70.

—— Cardellach, E., and Ayora, C. (1988) Génesis del filón Atrevida (Tarragona): Datos de inclusiones fluídas e isótopos de azufre. *Bol. Soc. Esp. Min.*, **11**, 135–6.

De Ronde, C. E. J. and Blattner, P. (1988) Hydrothermal alteration, stable isotopes and fluid inclusions of the Golden Cross epithermal Gold–Silver Deposit, Waihi, New Zealand. *Econ. Geol.*, **83**, 895–917.

Dill, H. (1988) Geologic setting and age relationship of fluorite–barite mineralization in Southern Germany with special reference to the Late Paleozoic unconformity. *Mineral. Deposita*, **23**, 16–23.

Fehn, U. (1985) Postmagmatic convection related to HHP in granites of SW England. In *HHP granites, hydrothermal circulation and ore genesis,* Inst. Min. Met., London, 99–112.

Fournier, R. O. (1985a) The behaviour of silica in hydrothermal solutions. *Rev. Econ. Geol.*, **2**, 45–63.

—— (1985*b*) Carbonate transport and deposition in the epithermal environment. Ibid., **2**, 64–72.

Giggenbach, W. F. (1988) Geothermal solute equilibria. Derivation of Na–K–Mg–Ca geoindicators. *Geochim. Cosmochim. Acta*, **52**, 2749–65.

Hedenquist, J. W. and Henley, R. W. (1985) The importance of CO_2 freezing point measurement of fluid inclusions: evidence from active geothermal systems and implications for epithermal ore deposition. *Econ. Geol.*, **80**, 1379–406.

Helgeson, H. C. (1969) Thermodynamics of hydrothermal systems at elevated temperatures and pressures. *Am. J. Sci.*, **267**, 729–804.

—— Delany, J. M., Nesbitt, H. W., and Bird, D. K. (1978) Summary and critique of the thermodynamic properties of rock-forming minerals. Ibid., **278**-A, 229 pp.

—— Kirkham, D. H., and Flowers, G. C. (1981) Theoretical prediction of the thermodinamic behavior of aqueous electrolytes at high pressure and temperature: IV: Calculation of activity coefficients, osmotic coefficients and apparent molal properties to 5 kb and 600 °C. Ibid., **281**, 1241–516.

Henley, R. W., Truesdell, A. H., and Barton, P. B. (1984) Fluid–mineral equilibria in hydrothermal systems. *Rev. Econ. Geol.*, **1**, 265 pp.

Ibarrola, E., Villaseca, C., Vialette, Y., Fuster, J. M., Navidad, M., Peinado, M., and Casquet, C. (1988) Dating of Hercynian granites in the Sierra de Guadarrama (Spanish Central System). In *Geología de los granitoides y rocas asociadas del Macizo Hespérico*, ed. Rueda, Madrid, 377–83.

Lhegu, J., Jebrak, M., Touray, J. C., and Ziserman, A. (1982) Les filons de fluorite et de barytine du Massif Central français. *Bull. BRGM.*, (2), II–2, 165–77.

Locutura, J. and Tornos, F. (1985) Consideraciones sobre la metalogenia del sector medio del Sistema Central Español. *Rev. R. Acad. Ciencias Fis. Exac. Nat.*, **59**, 589–623.

—— —— (1987) Aspectos genéticos de las mineralizaciones de F (Ba–Pb) de área de Colmenar de Arroyo (Sistema Central Español). *Bol. Geol. Min.*, **98**, 680–94.

—— —— Florido, P., and Baeza, L. (1990) Metallogeny of Spanish Ossa Morena Zone. In *Premesozoic evolution of Iberia*, Springer Verlag, 321–30.

Martinez, J., Oyarzun, R., Mayor, N., Lunar, R., and Vindel, E. (1988) Mineralizaciones de la Sierra de Guadarrama. Aplicación del modelo epitermal. *Bol. Soc. Esp. Min.*, **11**, 27–34.

Mayor, N., Lunar, R., and Oyarzun, R. (1988) Mineralizaciones filonianas de barita–fluorita–cuarzo–(metales de base–Ag) del sector centro-occidental del Sistema Central Español). Ibid., **11**, 137–9.

McKibben, M. A., Andes, J. P., and Williams, A. E. (1988) Active ore formation at a brine interface in metamorphosed deltaic lacustrine sediments: The Salton Sea geothermal system, California. *Econ. Geol.*, **83**, 511–23.

Melgarejo, J. C. and Ayora, C. (1985) La Mina Atrevida (Ba, F, Pb, Zn, As, Ni, Ag), Cadenas Costero Catalanas: Un ejemplo de filón triásico de zócalo-cobertera. *Rev. Inv. Geol.*, **40**, 87–102.

Nicholls, J. and Crawford, M. L. (1985) FORTRAN programs for calculation of fluid properties from the microthermometric data on fluid inclusions. *Computers Geosci.*, **11**, 619–45.

Ortega, L., Vindel, E., and Lunar, R. (1988) Estudio de los filones de baritina intragraníticos del sector Cenicientos–Cadalso de los Vidrios (Sistema Central). *Bol. Soc. Esp. Min.*, **11**, 89–99.

Patterson, D. J., Ohmoto, H., and Solomon, M. (1981) Geological setting and genesis of cassiterite-sulfide mineralization at Renison Bell, Western Tasmania. *Econ. Geol.*, **76**, 393–438.

Reed, M. H. and Spycher, N. F. (1985) Boiling, cooling and oxidation in epithermal systems: A numerical model approach. *Rev. Econ. Geol.*, **2**, 249–71.

Richardson, C. K. and Holland, H. D. (1979) The solubility of fluorine in hydrothermal solutions, an experimental study. *Geochim. Cosmochim. Acta*, **43**, 1313–25.

Roedder, E. (1984) Fluid inclusions. *Rev. Mineralogy*, **12**. Miner. Soc. Amer. 644 pp.

Routhier, P. (1983) *Where are the metals for the future?* BRGM, Paris, 397 pp.

Seward, T. M. and Barnes, H. L. (1987) Ore mineral solubility, transport and deposition, NATO ASI, *Geochemistry of hydrothermal ore processes,* Salamanca (in press).

Thibicroz, J. (1982) Typologie des gites de fluorine. Repartition des gisements en France et dans les regions voisines. *Bull. BRGM* (2), II–4, 437–99.

Tornos, F. (1990) *Evolución petrológica y metalogénica de los skarns del Sistema Central Español.* Doctoral Thesis. Universidad Complutense de Madrid, 487 pp.

Tritlla, J. and Cardellach, E. (1988) Filones de Pb–Ba en el paleozoico del área de Martorell (Barcelona). *Bol. Soc. Esp. Min.*, **11**, 167–72.

Ubanell, A. G. (1981) Características principales de la fracturación tardihercínica en un segmento del Sistema Central Español. *Cuad. Geol. Iber.*, **7**, 541–605.

Ulrich, M. R. and Bodnar, R. J. (1988) Systematics of stretching of fluid inclusions II. Barite at 1 atm confining pressure. *Econ. Geol.*, **83**, 137–46.

Vindel, E. (1980) *Estudio mineralógico y metalogénico de las mineralizaciones de la Sierra de Guadarrama.* Doctoral Thesis. Universidad Complutense de Madrid, 249 pp.

Walshe, J. L. (1986) A six component chlorite solid solution model and the conditions of chlorite formation in hydrothermal and geothermal systems. *Econ. Geol.*, **81**, 681–703.

[*Manuscript received 20 December 1989; revised 15 November 1990*]